[32] Young S, Wong M, Tabata Y, Mikos AG. Gelatin as a delivery vehicle for the controlled release of bioactive molecules. J Control Release 2005;109:256–74.
[33] Okada H, Yamamoto M, Heya Y, Inoue Y, Kamei S, Ogawa Y, et al. Drug delivery using biodegradable microspheres. J Control Release 1994;28:121–9.
[34] Niwa T, Takeuchi H, Hino T, Kunou N, Kawashima Y. Preparation of biodegradable nanospheres of water-soluble and insoluble drugs with D,L-lactide/glycolide copolymer by a novel spontaneous emulsification solvent diffusion method, and the drug release behavior. J Control Release 1993;25: 89–98.
[35] Higaki M, Ishihara T, Izumo N, Takatsu M, Mizushima Y. Treatment of experimental arthritis with poly(D, L-lactic/ glycolic acid) nanoparticles encapsulating betamethasone sodium phosphate. Ann Rheum Dis 2005;64:1132–6.
[36] Sakai T, Kohno H, Ishihara T, Higaki M, Saito S, Matsushima M, et al. Treatment of experimental autoimmune uveoretinitis with poly(lactic acid) nanoparticles encapsulating betamethasone phosphate. Exp Eye Res 2006; 82:657–63.
[37] Husmann KR, Morgan AS, Girod DA, Durham D. Round window administration of gentamicin: a new method for the study of ototoxicity of cochlear hair cells. Hear Res 1998; 125:109–19.
[38] Hatano T, Miyamoto S, Kawakami O, Yamada K, Hashimoto N, Tabata Y. Acceleration of aneurysm healing by controlled release of basic fibroblast growth factor with the use of polyethylene terephthalate fiber coils coated with gelatin hydrogel. Neurosurgery 2003;53:393–400.
[39] Park H, Temenoff JS, Holland TA, Tabata Y, Mikos AG. Delivery of TGF-beta1 and chondrocytes via injectable, biodegradable hydrogels for cartilage tissue engineering applications. Biomaterials 2005;26:7095–103.
[40] Alzamil KS, Linthicum FH Jr. Extraneous round window membranes and plugs: possible effect on intratympanic therapy. Ann Otol Rhinol Laryngol 2000;109:30–2.

# Tissue engineeringの最前線

## ——生体組織の再生誘導治療を実現する医工学材料技術

Frontier of tissue engineering——biomedical materials and technologies to realize induction therapy of tissue regeneration

田畑泰彦
Yasuhiko TABATA
京都大学再生医科学研究所生体組織工学研究部門生体材料学分野

◎細胞を利用した生体組織の再生誘導治療(＝再生医療)には，細胞が増殖・分化できるための適当な環境(場)をつくり与えることが必要不可欠である．この再生誘導の場を構築する医工学技術・方法論が tissue engineering である．Tissue engineering は生体材料(biomaterial)学がその基盤となっている．生体組織を構成する細胞外マトリックス，細胞，生体シグナル因子を利用するために，それぞれに対応した tissue engineering の役割がある．細胞を立体的に配置させ，細胞の増殖・分化を促進，あるいは再生のじゃまになる細胞や組織の侵入から再生誘導の場を確保するための技術，体内で不安定な細胞増殖因子や遺伝子を利用するためのドラッグデリバリーシステム(DDS)技術，必要な細胞を分離・増殖させるための技術などの研究開発が大切である．本稿では再生医療における tissue engineering の最前線と将来の方向性について述べる．

Key word：tissue engineering，生体材料，生体シグナル因子，ドラッグデリバリーシステム(DDS)

### 再生誘導治療(＝再生医療)に必要な tissue engineeringと再生医学

人工臓器が完全には体になじまず，また，補助できる機能が単一であること，あるいは移植組織・臓器の慢性的な不足，免疫抑制剤の服用による副作用などの点から，これまでに多くの患者の生命を救ってきた再建外科治療と臓器移植との二大先端外科治療・技術，方法論の限界がみえてきている．このような状況のなかで新しく考えられているのが，イモリのしっぽが再生する現象をヒトで誘導し，治療に役立てようとする再生誘導治療(一般には再生医療とよばれている)である．再生医療は長所・短所もあり，けっしてオールマイティーではないが，これまでの先端外科治療の欠点を補い，従来治療法の適用拡大を可能とするだけでなく，新しい治療法を提案する可能性もあるため，第三の治療法としておおいに期待される．

この再生医療が現実味をおびてきた背景には主として２つの研究分野の進歩がある．１つ目は，再生誘導現象にかかわる細胞とその増殖・分化のための周辺環境としての細胞外マトリックスおよび生体シグナル因子(細胞増殖因子や遺伝子など)に関する基礎生物医学研究(再生医学とよばれる)である．２つ目が tissue engineering(生体組織工学)である．これは生体組織(tissue)の再生誘導を手助けするための周辺環境(場)をつくり与える医工学(engineering)技術・方法論であり，人工臓器の開発研究と臨床実績とを築き上げた生体材料(biomaterial)学がその基礎となっている[1]．

### 生体組織の再生誘導の場をつくる tissue engineering

再生医療の発想は何であったのか．生体吸収性高分子からなる三次元フェルト材料内で肝細胞を培養し，得られた肝臓様構造物を移植肝の代りとして利用できないかと考えた．これが再生医療のはじまりである．細胞とその周辺環境(フェルトからなる)とを組み合わせ，細胞のもつ生体組織の再

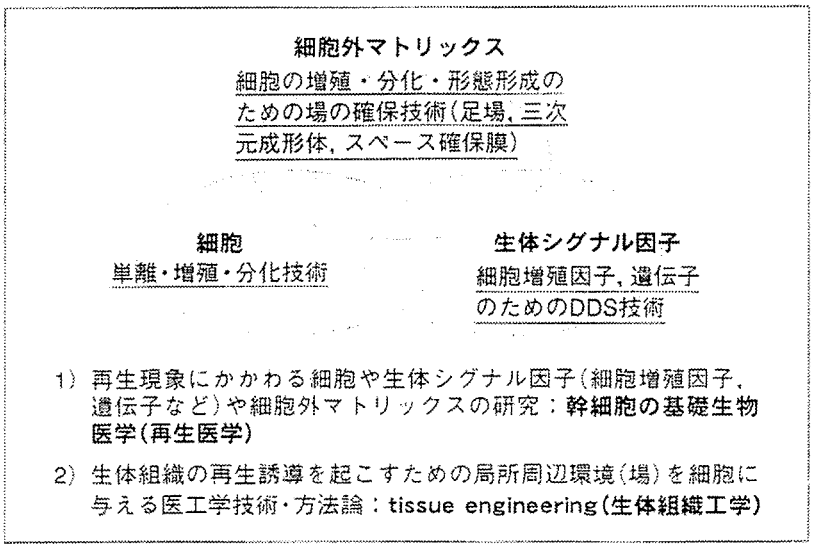


**図 1　再生医療を実現するためには再生医学とtissue engineeringの両方が必要である**

細胞外マトリックス，細胞，生体シグナル因子に対応した tissue engineering 技術がある．下線を引いた部分が tissue engineering の役割を示す．

生誘導力に基づく新しい治療方法の提案であった．用いる細胞が患者由来のものであれば，得られた肝臓様構造物に対する免疫拒絶反応もなく，かつ材料は分解消失するため異物反応もなく，理想的な治療法となる．増殖分化能力の高い幹細胞や前駆細胞を体内に投与するだけでは，生体組織・臓器の再生誘導の望めない場合が多い．これは現時点において細胞の増殖や分化に不可欠である局所周辺環境に関する科学的知見が乏しく，細胞の分化の制御がきわめて難しいからである．

それでは体内の仕組みがわからなければ，新しい治療法が実現できないのであろうか．答えは否である．今日の疾病の治療は病因の解明を待って行われるのではなく，むしろそのような例はわずかである．これは，生体が本来，自己再生修復能力をもっているからである．サイズの小さな傷であれば，なにも手を加えなくても自然と修復していく．しかし，傷のサイズが大きい，あるいは生体条件の悪い場合には再生修復能力を高めるための工夫が必要となる．その工夫のひとつが tissue engineering である．自然治癒力をサポートして病気を治す，体にやさしい治療法である．現在の医療は生物医学だけではなく，多くの研究領域の研究開発成果のうえに成り立っていることはいうまでもない[1]．治療学のひとつである再生医療も同じである．再生医療の目的は新しい治療法の確立であり，発生・分化の解明ではない．基礎生物医学としての発生・分化の解明も重要であるが，それが直接には患者の治療(つまり再生医療)につながらないことも多い．

## Tissue engineeringの最前線と今後の方向性

再生医療の目的は，欠損した生体組織の再生誘導と障害臓器の機能の代替による病気の治療である．この目的が行われる場所により，生体外と生体内とに分けられる．細胞培養技術により細胞を増殖・分化させ，生体組織様の構造物をつくったり細胞と生体材料とを組み合わせて臓器機能を代替する試み(生体外 tissue engineering)が行われてきたが，現在の細胞培養技術，基礎生物医学の知見のみでは生体組織の再生誘導の場を生体外でつくることはきわめて難しい．これに対して，再生誘導の仕組みが完全に解明されていなくても生体由来の必要な物質を必要な部位に自動的に供給できる工夫をすれば，生体内における再生誘導は実現できる[1-4]．その基本戦略は，生体組織を構成する3要素である細胞外マトリックス，細胞，および生体シグナル因子を用い，それに生体材料を組み合わせて生体組織の再生誘導のための場をつく

ることである．それぞれの構成要素の基礎生物医学(再生医学)に対応する tissue engineering があり(図 1)，以下に，その役割と具体例について述べる．

Tissue engineering の第 1 の役割は生体組織の再生誘導のための場の確保である[5,6]．体内では血液細胞と癌細胞以外のほとんどすべての細胞は細胞外マトリックス(天然の足場)と相互作用して生存し，その生物機能を発揮している．生体組織が欠損すると，細胞とともにこのマトリックスまでもなくなっている．そこで，組織の再生誘導のためには細胞を与えるだけでは十分でなく，人工的に再生誘導の場を欠損部に与えることが必要となる．たとえば，細胞を立体的に配置させ，その接着・増殖・分化促進のための三次元成形材料(一般に足場；scaffold とよばれる)を用いる[6]．材料の残存が生体組織の再生を物理的に邪魔しないような適度な生体吸収性，細胞が材料内部まで入っていきやすく，また，細胞への酸素，栄養の供給と老廃物の排除のための多孔性などが足場の必須条件である．すでに，生体吸収性のコラーゲンスポンジとポリグリコール酸メッシュなどを用いるだけで皮膚真皮層，食道，気管，脳硬膜，末梢神経などの生体組織の生体内再生修復が実現でき[7]，すでに臨床研究による治療効果が確認されている．たとえば，力学的補強した足場細胞の再生誘導能を高めることがわかっている[8]．生体吸収性高分子チューブを患者の骨髄細胞とともに肺動脈の欠損部位にグラフトしたところ，チューブ内で細胞が増殖・分化して血管構造が再生され，それとともにチューブは分解消失した[9]．このように，現在，生体吸収性材料を適材適所に利用することにより生体組織の再生誘導が可能になっている．Tissue engineering は生体材料学のひとつの発展型である．今後，細胞の増殖・分化のための分子レベルでのメカニズムが解明されれば，それらの key 分子を組み込んだ人工の細胞外マトリックスのデザインも可能となっていくであろう．

再生誘導の場を確保するためのもうひとつのアプローチがある．それは，欠損部への線維性組織の侵入充填を防ぐために膜を用いる方法である．この発想はすでに GTR(guided tissue regeneration)膜，GBR(guided bone regeneration)膜として実用化され，歯周組織の再生治療が行われている[10]．また，生体吸収性高分子チューブを末梢神経の欠損部に挿入することで，末梢神経の再生治療は臨床的にも可能となっている[11]．

生体組織の再生誘導には 2 つのアプローチがある．ひとつは tissue engineering を利用した再生誘導法であり，もうひとつが，増殖・分化能力の高い細胞の直接移植(細胞移植治療)である．後者の治療法では質の高い多くの幹細胞や前駆細胞を迅速に得ることが不可欠である．そこで，効率よく細胞を単離・増殖させるための培養技術が必要となる．三次元成形材料，培養装置(バイオリアクタ)などを活用することによって生体内環境を模倣し，幹細胞の増殖効率を高めるための材料，技術，方法論の研究開発が急がれる．

生体シグナル因子に対応する tissue engineering も必要である．生体組織のもつ潜在的な再生誘導能力が乏しい場合には，場の確保技術だけでは再生誘導は期待できない．このような場合には細胞を利用する方法と細胞の増殖・分化を促す生体シグナル因子を利用する 2 つのアプローチがある．一般に，細胞増殖因子や遺伝子などの生体因子の生体内寿命は短く不安定であり，必要な因子を単に水に溶かして必要部位に投与するだけでは，期待する組織再生誘導効果は得られない．そこで，再生誘導の場において，必要な因子を必要な濃度を必要な期間にわたって作用させるための工夫が必要である．このための技術・方法論がドラッグデリバリーシステム(DDS)である(「サイドメモ」参照)[12]．その目的は持続的放出(徐放)化，生体内寿命の延長，吸収促進，あるいはターゲティングなどであるが，いずれの目的も再生医療に利用できる．たとえば，生体吸収性材料を利用して細胞増殖因子を再生の場で徐放すれば，細胞の増殖分化が高まり，自己組織の再生が促される[2-5,12]．この徐放化システムは，単独あるいは細胞とともに足場や再生誘導の場の確保技術と組み合わせて生体組織の再生誘導に用いられている．DDS はこれまでの研究開発の経緯から薬物治療のイメージが強く，再生医療とは無関係であると考えられてきたが，生体内で不安定で，しかも作用部位の特

異性もない細胞増殖因子，遺伝子などを利用するかぎり，DDS 技術は不可欠である[12]．

塩基性線維芽細胞増殖因子(bFGF)などの細胞増殖因子の徐放化[13]によってさまざまな生体組織の再生誘導が可能となっている[2,3,7,12]．たとえば，イヌ心筋梗塞モデルあるいは糖尿病ウサギの下肢虚血モデルの筋肉内へ bFGF 含浸ゼラチンヒドロゲル粒子を投与したところ，血管新生が誘導された[14,15]．すでに，bFGF 徐放化システムを用いた下肢虚血疾患に対する血管誘導治療の臨床研究が開始され，よい成績が得られている．bFGF は血管だけでなく，骨組織の再生誘導も促進することが知られている[16]．bFGF 含浸ゼラチンヒドロゲルを利用した骨と血管との同時再生誘導が可能になっている[17]．また，骨・軟骨組織や脂肪組織の再生誘導，神経，毛髪の伸長なども細胞増殖因子の徐放化により実現されている[3]．

複数の細胞増殖因子を徐放することもできる．ゼラチンヒドロゲルを用いた bFGF とトランスホーミング増殖因子(TGF)$\beta$1 との徐放化による骨再生誘導の相乗効果[18]，bFGF と肝細胞増殖因子との徐放化による新生血管の成熟度の向上[19]，血小板中に含まれる複数の細胞増殖因子の徐放化による骨再生修復などが可能になっている[20]．

細胞移植治療，あるいは機能細胞を用いた臓器機能の代替治療では体内に移植された細胞の生存，その機能維持のために酸素・栄養の供給が必要不可欠である．bFGF 徐放化による新生血管誘導は，骨髄由来未分化間葉系幹細胞，Langerhans 島，肝細胞，あるいは腎尿細管上皮細胞などの生物機能を向上させ，優れた治療効果[21-23]を実現している．加えて，培養表皮-真皮 2 層皮膚様構造物の生着率も向上することがわかっている[24]．

## おわりに

再生医療は生体吸収性材料を用いた医工学的な工夫を加えることで細胞を増殖・分化させ，生体組織の再生を誘導するという tissue engineering がその基本になっている．これまでの生体材料とは違って，長期間にわたって体内で残存することがなければ，材料に対する生体反応は問題とはならない．生体の再生修復過程の邪魔にならず，かつ細胞の増殖・分化を support する生体吸収性材料が設計・利用できるようになってきた現在，生体組織の再生誘導は現実のものとなっている．生体吸収性の足場材料のみを用いた生体組織の再生誘導治療，bFGF の徐放化技術による血管，骨，皮膚真皮などの再生誘導治療は臨床研究がはじまり，よい治療効果を得ている．加えて，獣医学領域においても骨などの生体組織の再生医療はすでに現実のものとなっている[25,26]．

体内の欠損部に外科的に再生の場をつくり再生を誘導する，これまでの“外科的再生医療”アプローチとは異なり，線維化組織を消化吸収することで体内に再生誘導の場を確保し，周辺組織の再生誘導ポテンシャルを介して難治性慢性疾患の治療を行うという“内科的再生医療”の試みもはじまっている[5,27]．遺伝子の直接投与によるこれまでの遺伝子治療に加えて，遺伝子改変により機能増強された幹細胞を用いる細胞移植治療も期待されている[28]．幹細胞内でのプラスミド DNA の徐放化によってウイルスに匹敵する高いレベルの細胞の遺伝子改変とそれらの細胞による高い細胞治療効果が達成されている．今後，tissue engineering

**サイドメモ　ドラッグデリバリーシステム**

ドラッグデリバリーシステム(drug delivery system：DDS)とは，Drug(何らかの作用を与える物質の総称)の効果を最大限に発揮させることを目的とした，drug と組み合わせる材料，技術，方法論の研究開発分野．これまで drug＝治療薬ととらえられてきたことから，治療効果を高めるための薬学・製剤学の分野であると考えられてきた．しかし，drug を予防薬，診断薬と考えれば，DDS は予防・診断効果を高めるための技術となる．DDS を用いれば，プラスミド DNA，siRNA，デコイ DNA などの細胞への取込み，発現も高まる．また，化粧品の成分としての美白剤，UV カット剤にも DDS 概念は適用できる．このように drug を徐々に放出(徐放)，drug の水可溶化と安定化，drug の吸収促進，および drug の作用部位へのターゲティングなどの DDS は，医療(治療，予防，診断)だけにとどまらず，生物医学研究，ヘルスケアなどにも広く活用できる自然科学に対する普遍的な基盤技術である．

による生体組織の再生誘導と臓器機能の代替の研究開発はますます活発になり，対象となる組織・臓器も増えていくであろう．再生組織の診断法の研究開発を急がなければならない．材料を活用した再生医療であれば，事業化，実用化も夢ではない．新しいアイデア，新しい技術・方法論を積極的に医療へ組み入れていく社会的システムが欲しいものである．

## 文献


1) 田畑泰彦(編)：再生医療へのブレイクスルー　その革新技術と今後の方向性．メディカルドゥ，2004.
2) 田畑泰彦(編)：ここまで進んだ再生医療の実際．羊土社，2003.
3) Tabata, Y.：*Tissue Engineering*, **9**：S5-S15, 2003.
4) 田畑泰彦：治療学，**38**：116-121，2004.
5) Tabata, Y.：*Drug Discovery Today*, **10**：1639-1646, 2005.
6) 田畑泰彦：*THE BONE*，**17**：24-29，2003.
7) 田畑泰彦：*Biotherapy*，**18**：91-105，2004.
8) Itoh, M. et al.：*Tissue Engineering*, **10**：818-824, 2004.
9) Shin'oka, T. et al.：*N. Engl. J. Med.*, **344**：532-533, 2001.
10) Dahlin, C. et al.：*Int. J. Oral Maxillofac. Implants*, **4**：19-25, 1989.
11) Inada, Y. et al.：*Pain*, **117**：251-258, 2005.
12) 田畑泰彦(編)：ドラッグデリバリーシステム　DDS技術の新たな展開とその活用法．遺伝子医学別冊，2003.
13) Tabata, Y. et al.：*Adv. Drug Delivery Rev.*, **31**：287-301, 1998.
14) Yamamoto, M. et al.：*Artif. Organs*, **27**：181-184, 2003.
15) Nakajima, H. et al.：*J. Artif. Organs*, **7**：58-61, 2004.
16) Tabata, Y. et al.：*J. Neurosurg.*, **91**：851-856, 1999.
17) Iwakura, A. et al.：*Circulation*, **102**：Ⅲ307-Ⅲ311, 2000.
18) Tabata, Y. et al.：*J. Biomater. Sci. Polym. Ed.*, **11**：891-901, 2000.
19) Iwakura, A. et al.：*Heart Vessels*, **18**：93-99, 2003.
20) Hokugo, A. et al.：*Tissue Eng.*, **11**：1224-1233, 2005.
21) Balamurugan, A. N. et al.：*Pancreas*, **26**：103-104, 2003.
22) Ogawa, K. et al.：*Cell Transplant.*, **10**：723-729, 2001.
23) Saito, A. et al.：*J. Am. Soc. Nephrol.*, **14**：2025-2032, 2003.
24) 佐生泰美・他：熱傷，**29**：24-30，2003.
25) 岸上義弘・他：*Companion Animal Practice*，**176**：17-35，2004.
26) 岸上義弘・他：*Companion Animal Practice*，**178**：32-60，2004.
27) 山本雅哉・他：*Drug Delivery System*，**20**：110-117，2005.
28) 永谷憲蔵：*Drug Delivery System*，**20**：105-109，2005.


*　　*　　*

*The Laryngoscope*
Lippincott Williams & Wilkins, Inc.


# Age-Dependent Degeneration of the Stria Vascularis in Human Cochleae

Teruhisa Suzuki, MD; Yukio Nomoto, MD; Takayuki Nakagawa, MD, PhD; Naofumi Kuwahata, MD; Hiroshi Ogawa, MD, PhD; Yukie Suzuki, MD, PhD; Juichi Ito, MD, PhD; Koichi Omori, MD, PhD

***Objective:*** **Aging is a common cause of acquired hearing impairments. This study investigated age-related morphologic changes in human cochleae, with a particular focus on degeneration of the stria vascularis (SV) and the spiral ganglion (SG).** ***Study Design:*** **Retrospective case review.** ***Methods:*** **The study group comprised 91 temporal bones from individuals aged 10 to 85 years who had no history or audiometric findings suggestive of specific causes of cochlear degeneration. We quantified the SV and SG atrophy at each cochlear turn using morphometric measurements. Correlations of the SV and SG atrophy with age, audiometric patterns of hearing loss, and auditory thresholds were statistically investigated.** ***Result:*** **The SV and the SG both showed a tendency for progressive atrophy to develop with age. However, statistically significant correlations were observed between aging and SV atrophy only in the apical and basal cochlear turns. These findings were consistent with those reported previously in gerbils. No significant correlations were detected between SV or SG atrophy and audiometric findings.** ***Conclusion:*** **SV atrophy appears to be the most prominent anatomic characteristic of aged human cochleae.** ***Key Words:*** **Aging, atrophy, cochlea, human, pathology, spiral ganglion, stria vascularis.**
***Laryngoscope,*** **116:1846–1850, 2006**

## INTRODUCTION

Age-related degenerative hearing loss (HL) is known as presbycusis and is the most common cause of hearing impairments in adults. As human populations age, this condition is expected to become more prevalent. At present, the therapeutic options for presbycusis are limited to the use of hearing aids. Until recently, mammals were thought to be unable to regenerate cochlear elements; however, recent medical advances have highlighted the potential for the regeneration of cochlear elements through gene or cell therapy.[1,2] In addition, animal experiments have identified various molecules that might be applied therapeutically to protect cochlear cells.[3–5] Although these experimental findings have not yet been applied clinically, they could help to establish novel therapeutic strategies for presbycusis.

It is crucial to determine the cells or tissues in aged cochleae that should be targeted by future therapies. Several animal experiments have indicated that degeneration of the stria vascularis (SV) or the spiral ganglion (SG) is a prominent pathologic, age-related cochlear change.[6–12] However, studies on human temporal bones will be necessary to confirm the precise targets for therapeutic strategies. Previous research has demonstrated several age-related histopathologic changes in human cochleae.[13–18] However, the general features of aged cochleae have not yet been established for humans. This is partly because the subjects of previous studies have tended to include patients with ear diseases or profound hearing impairments. In such cases, cochlear degeneration might be caused by ototoxic pathogens or an ototoxic internal environment, which makes it difficult to distinguish the specific abnormalities caused by aging. Recently, two articles[19,20] carefully excluded temporal bones of subjects with a history of ear diseases. However, previous authors have examined insufficient numbers of human temporal bones to allow the general histopathologic characteristics of aged cochleae to be determined. To address these issues, we conducted a quantitative analysis of age-related histopathologic changes of the SV and SG using a large sample of human temporal bones.

From the Department of Otolaryngology (T.S., Y.N., N.K., H.O., Y.S., K.O.), Fukushima Medical University, School of Medicine, Fukushima, and the Department of Otolaryngology–Head and Neck Surgery (T.N., J.I.), Kyoto University Graduate School of Medicine, Kyoto, Japan.

Editor's Note: This Manuscript was accepted for publication June 14, 2006.

This study was supported by Health and Labour Science Research Grants for Research on Sensory and Communicative Disorders from the Ministry of Health, Labour, and Welfare, Japan.

Send correspondence to Dr. Koichi Omori, Department of Otolaryngology, Fukushima Medical University, School of Medicine, Hikarigaoka 1, Fukushima 960-1295, Japan. E-mail: omori@fmu.ac.jp; or Dr. Takayuki Nakagawa, Department of Otolaryngology–Head and Neck Surgery, Graduate School of Medicine, Kyoto University, Kawaharacho 54, Shogoin, Sakyo-ku, 606-8507 Kyoto, Japan. E-mail: tnakagawa@ent.kuhp.kyoto-u.ac.jp

**DOI: 10.1097/01.mlg.0000234940.33569.39**

## MATERIALS AND METHODS

### *Subjects*

In total, 91 temporal bones from a collection of 1,278 specimens held at the Department of Otolaryngology, Fukushima Medical University, Japan, were selected for morphometric analyses. We used unilateral temporal bones from 91 different patients. We excluded subjects with history of ear diseases or ototoxic drug use by reviewing their medical records. Pure-tone audiometry had been performed within 24 months of death for all of the selected subjects. Individuals with audiograms showing a characteristic 4,000 Hz dip (that is, thresholds greater than 25 dB at 2 and 8 kHz), which indicates noise-induced HL, were excluded from the study. The subjects ranged in age from 10 to 85 years, with a mean and standard deviation of 59.7 and 16.8 years, respectively.

For all of the chosen subjects, the temporal bones had been removed within 48 hours of death and were fixed with 10% formalin. After decalcification, the temporal bones were embedded in celloidin and serially sectioned in a horizontal plane at a thickness of 20 $\mu$m. Every 10th section was stained with hematoxylin-eosin. The adjacent two mid-modiolus sections were subjected to morphometric assessments. In all the specimens used in this study, we found no postmortem degeneration in the SG and SV.

### *Audiometric Classification*

The audiometric hearing-loss patterns were determined based on the air-conductance thresholds at frequencies of 250, 500, 1,000, 2,000, 4,000, and 8,000 Hz. All audiometric patterns with a threshold less than 25 dB were considered to be normal. A flat pattern was defined as HL with a threshold greater than 25 dB and a maximum threshold difference of 20 dB between frequencies of 250 and 8,000 Hz. A high–tone-loss pattern was defined as HL with a threshold greater than 25 dB at 4,000 and 8,000 Hz and a difference in thresholds between 2,000 and 4,000 Hz with an increase of more than 20 dB. A descending pattern was defined as HL with a threshold greater than 25 dB at 2,000, 4,000, and 8,000 Hz and a difference in thresholds between 2,000 and 4,000 Hz with an increase of less than 20 dB. In addition to the audiometric hearing-loss patterns, the average bone-conductance thresholds were determined at the following five frequencies: 250, 500, 1,000, 2,000, and 4,000 Hz. This measure was used as an audiometric parameter.

### *Morphometric Assessments*

Morphometric assessments of the SV and the SG were performed for each cochlear turn at the mid-modiolar level. Images were acquired with a charged-coupling device camera connected to a personal computer. The areas of the SV, Rosenthal's canal, and cochlear turn were quantified by measuring their cut surfaces using Image/J software (http://www.nist.gov/lispix/imlab/prelim/dnld.html) (Fig. 1A). The total number of nuclei in Rosenthal's canal was counted for each cochlear turn. The ratio of the SV area (SV ratio) and the cell density of the SG (SG density) were used to reduce the variance caused by differences in cutting directions among the cochlear specimens. The SV ratio was determined by dividing the SV area by that of the cochlear turn. The SG density was determined by dividing the number of nuclei in Rosenthal's canal by its area.

### *Statistics*

The Pearson's correlation coefficient with Fisher's z transformation was used to examine the relationships between the following variables: age and average bone-conductance threshold; age and SV ratio or SG density for each cochlear turn; and average bone-conductance threshold and SV ratio or SG density. Differences in the SV ratio and SG density according to audiometric pattern were examined by a single factorial analysis of variance. A $P$ value less than .05 was considered statistically significant.

## RESULTS

Figure 2 shows the distribution of average bone-conductance thresholds according to age. A significant correlation was discovered between age and average auditory threshold (Fig. 2) ($r = 0.47$, $P < .0001$). This indicated that aging had a significant effect on the elevation of auditory thresholds among the members of the study group.

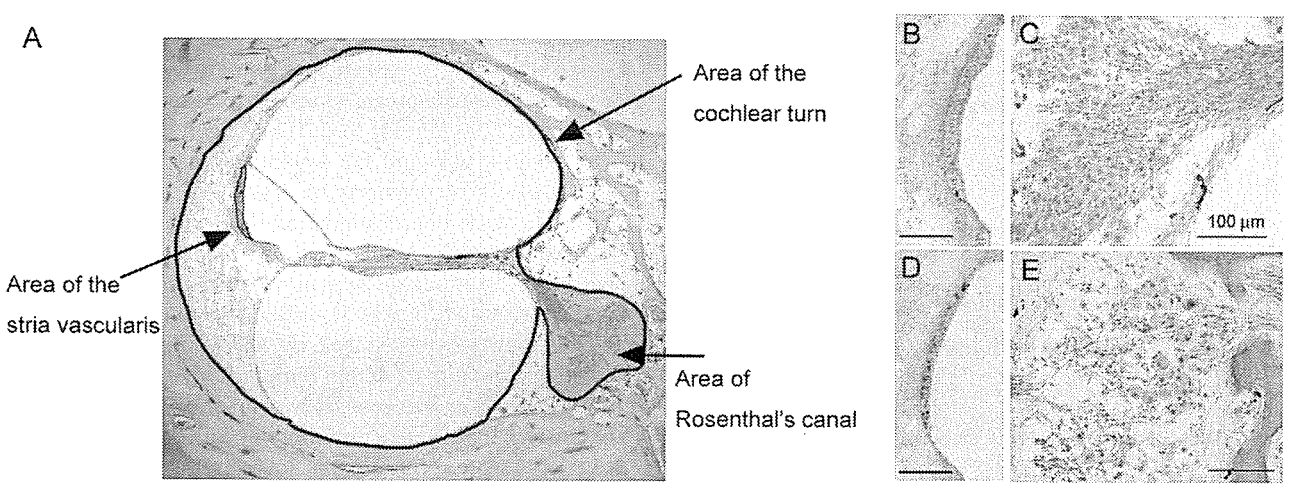


Fig. 1. Morphology of human cochleae. (A) Basal turn of cochlea of 38-year-old male. Area of cochlear turn (black line). Area of SV (dotted line). Area of Rosenthal's canal (gray section). (B) Stria vascularis (SV) of 19-year-old male showing no atrophic changes. (C) Spiral ganglion (SG) of a 37-year-old female exhibiting numerous neurons. (D) SV of 79-year-old male, which is more atrophic than that shown in B. (E) SG of a 77-year-old female, which shows relatively few neurons. Scale bars = 100 $\mu$m.

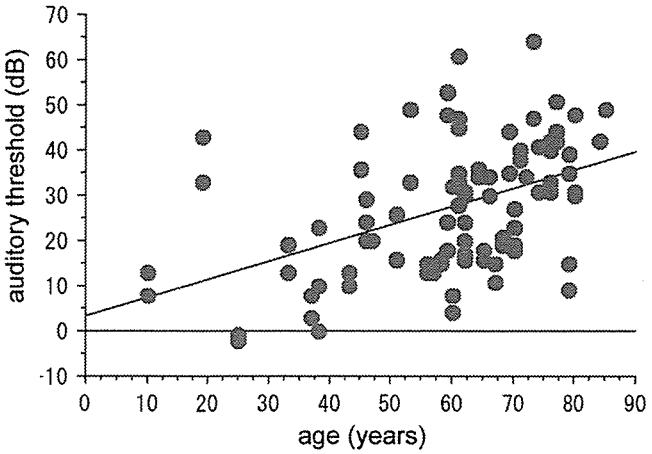


Fig. 2. Relationship between auditory threshold and age. x-axis shows age (years) and y-axis shows average bone-conductance thresholds (dB) at five frequencies (250, 500, 1,000, 2,000, and 4,000 Hz). Significant correlation was detected between average auditory threshold and age using the Pearson's correlation coefficient with Fisher's z transformation ($r = 0.47$, $P < .0001$).

Figure 3 shows the distribution of SV ratios for each cochlear turn according to age. A trend for the SV ratio to decrease with age was seen at every cochlear turn. A significant correlation between age and the SV ratio was found in the basal cochlear turn (Fig. 3A) ($r = -0.36$, $P = .0003$) and the apical cochlear turn (Fig. 3C) ($r = -0.23$, $P = .025$). By contrast, no significant correlation was observed in the middle cochlear turn (Fig. 3B). Figure 4 shows the distribution of SG densities for each cochlear turn according to age. Although the SG densities tended to decrease with age, none of the cochlear turns showed a statistically significant correlation between these variables.

The subjects of the present study were divided into four groups according to their audiometric patterns, as follows: 37 subjects showed a normal pattern, 25 subjects showed a descending pattern, 19 subjects showed a flat pattern, and 10 patients showed a high–tone-loss pattern. The means and standard errors of the SV ratios and SG densities for each audiometric-pattern group are shown in Figure 5. There were no significant differences in either the SV ratios or the SG densities among the audiometric pattern groups for each cochlear turn. We also examined the relationship between the average auditory threshold and the SV ratio or the SG density at each cochlear turn. No significant correlations were observed between these parameters.

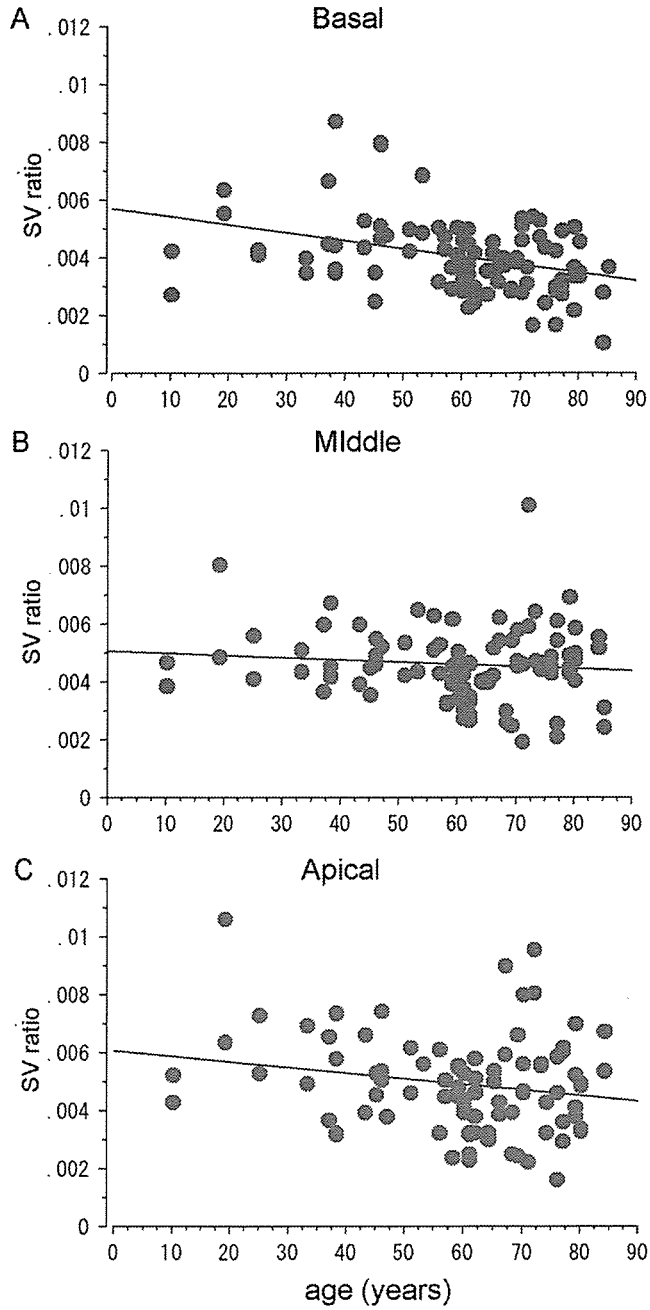


Fig. 3. Relationship between stria vascularis (SV) ratio and age in basal (A), middle (B), and apical (C) cochlear turns. x-axis shows age (yr) and y-axis shows SV ratio. Significant correlations between SV ratio and age were observed in basal and apical cochlear turns according to Pearson's correlation coefficient with Fisher's z transformation ($r = -0.36$, $P = .0003$ and $r = -0.23$, $P = .025$, respectively).

## DISCUSSION

The study group in the present analysis was screened to exclude individuals with hearing impairments caused by ototoxic pathogens other than aging by reviewing their medical records and pure-tone audiograms. Morphometric analysis of the 91 selected subjects revealed a significant correlation between auditory threshold and age, which indicated that aging had important effects on hearing performance, at least within our study population.

Our present findings demonstrated a significant correlation between SV atrophy and aging in human cochleae. This was consistent with previous findings reported for animal models. A series of studies on gerbils that were maintained under quiet conditions indicated that SV degeneration was the most prominent age-related histologic change in their cochleae.[6–8] Age-related SV degeneration in these gerbil models was

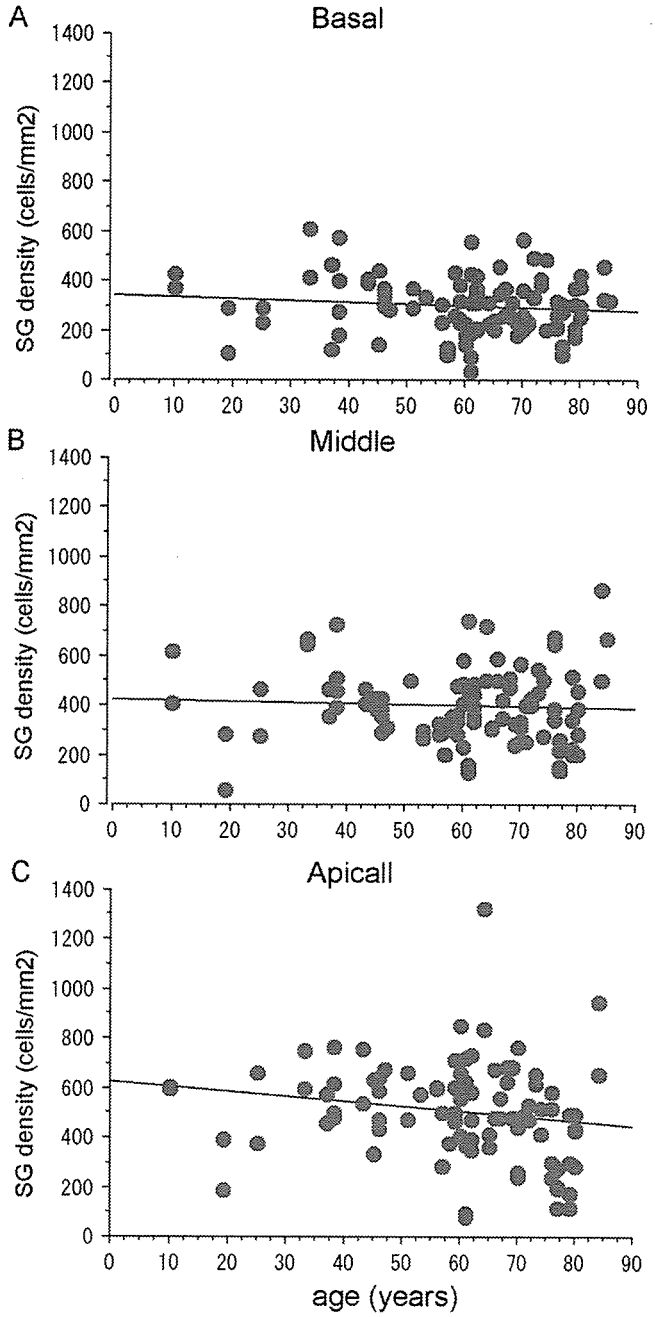


Fig. 4. Relationship between spiral ganglion (SG) density and age in basal (A), middle (B), and apical (C) cochlear turns. x-axis shows age (yr) and y-axis shows SG density. No significant correlations were observed between SG density and age in basal, middle, and apical cochlear turns.

usually found to originate in both the base and the apex of the cochleae. Our present results also identified significant aging effects on SV atrophy in the basal and apical portions of human cochleae. These findings support the hypothesis that SV degeneration is a morphologic characteristic of age-induced cochlear degeneration.

Schuknecht and Gacek[14] described degeneration of the SV as the most prominent morphologic characteristic of age-related HL based on their observations of human temporal bones. Recent morphometric analysis of human temporal bones[20] also supported this hypothesis. Nelson and Hinojosa[19] controversially concluded that SV atrophy was not specific to aged human cochleae with flat audiometric patterns of HL based on a precise morphometric analysis. The present study found no significant correlation between SV atrophy and audiometric patterns of HL or thresholds, although a significant correlation was detected between SV atrophy and aging. Previous studies on human subjects have indicated a poor correlation between audiometric patterns of HL and cochlear histopathology.[15–18] We therefore conclude that SV atrophy is an anatomic characteristic of age-induced cochlear changes but suggest that it is difficult to discern cochlear histopathology from conventional pure-tone audiometry.

The present study failed to find an age-dependent decrease in SG density. By contrast, several previous studies found significant correlations between aging and loss of SG neurons in both humans[15,20] and animal models.[11,12] These reports frequently noted a loss of SG neurons coupled with a loss of cochlear hair cells. Gates and Mills[18] showed that subjects experiencing loss of cochlear hair cells and SG neurons frequently had histories of noise exposure, indicating that these morphologic findings in human cochleae might have been induced by environmental noise. By contrast, in gerbils maintained under quiet conditions, which demonstrated age-dependent SV degeneration, loss of auditory nerve function was indicated by elevation of the compound action potentials of auditory nerves.[10] Recently, changes of the expression patterns of brain-derived neurotrophic factors have been demonstrated in the SG neurons of aged rats and gerbils.[21] This functional degeneration involved no significant loss of SG neurons. We therefore consider that the degeneration of SG neurons might be involved in age-related HL. However, these degenerative changes of the SG neurons cannot be detected by conventional histopathology of human temporal bones.

The present study failed to identify significant correlations between morphologic and audiometric findings in human subjects similar to those reported previously. One possible explanation for this discrepancy is that histologic findings obtained by conventional light microscopy cannot reveal changes in the functionality of cochlear elements, which might play critical roles in the process of age-induced HL.

## CONCLUSION

Our present analysis of 91 temporal bones indicates that SV atrophy is the most common histopathologic feature of aged human cochleae. This conclusion is supported by previous observations of aged animal models and human temporal bones. By contrast, age-dependent SG atrophy was not detected by conventional light microscopy in the present study, although several previous studies have indicated a correlation between functional degeneration of SG neurons and aging.

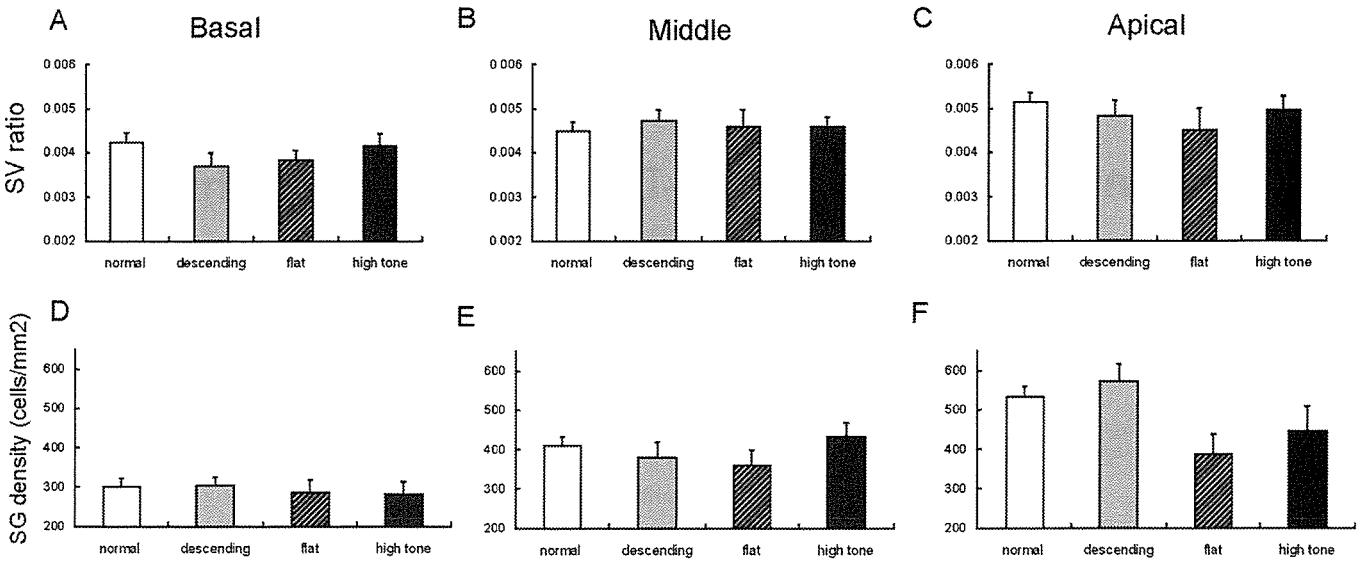


Fig. 5. Means and standard errors of stria vascularis (SV) ratios (A to C) and spiral ganglion (SG) densities (D to F) of experimental groups divided according to audiometric hearing-loss patterns. No significant differences in SV ratios or SG densities were found among experimental groups in the basal, middle, or apical cochlear turns.


## Acknowledgments

The authors thank Professor emeritus Iwao Ohtani for his establishment of temporal bone laboratory and Etsuko Sato for her technical contribution to this work.


## BIBLIOGRAPHY


1. Izumikawa M, Minoda R, Kawamoto K, et al. Auditory hair cell replacement and hearing improvement by *Atoh1* gene therapy in deaf mammals. *Nat Med* 2005;11:271–276.
2. Okano T, Nakagawa T, Endo T, et al. Engraftment of embryonic stem cell-derived neurons into the cochlear modiolus. *Neuroreport* 2005;16:1919–1922.
3. Seidman MD. Effects of dietary restriction and antioxidants on presbycusis. *Laryngoscope* 2000;110:727–738.
4. Ernfors P, Duan ML, El Shamy WM, Canlon B. Protection of auditory neurons from aminoglycoside toxicity by neurotrophin-3. *Nat Med* 1996;2:463–467.
5. Iwai K, Nakagawa T, Endo T, et al. Cochlear protection by local IGF-1 application using biodegradable hydrogel. *Laryngoscope* 2006;116:526–533.
6. Spicer SS, Schulte BA. Spiral ligament pathology in quiet-aged gerbils. *Hear Res* 2002;172:172–185.
7. Spiess AC, Lang H, Schulte BA, et al. Effects of gap junction uncoupling in the gerbil cochlea. *Laryngoscope* 2002;112: 1635–1641.
8. Schulte BA, Schmiedt RA. Lateral wall Na, K-ATPase and endocochlear potentials decline with age in quiet-reared gerbils. *Hear Res* 1992;61:35–46.
9. Schmiedt RA, Lang H, Okamura HO, Schulte BA. Effects of furosemide applied chronically to the round window: a model of metabolic presbycusis. *J Neurosci* 2002;22: 9643–9650.
10. Hellstrom LI, Schmiedt RA. Compound action potential input/output functions in young and quiet-aged gerbils. *Hear Res* 1990;50:163–174.
11. Shiga A, Nakagawa T, Nakayama M, et al. Aging effects on vestibulo-ocular responses in C57B/6 mice: comparison with alteration in auditory function. *Audiol Neurootol* 2005;10:97–104.
12. Keithley EM, Ryan AF, Woolf NK. Spiral ganglion cell density in young and old gerbils. *Hear Res* 1989;38:125–133.
13. Schuknecht HF. *Pathology of the Ear.* Cambridge, MA: Harvard University Press, 1974.
14. Schuknecht HF, Gacek MR. Cochlear pathology in presbycusis. *Ann Otol Rhinol Laryngol* 1993;102:1–16.
15. Suga F, Lindsay JR. Histopathological observations of presbycusis. *Ann Otol Rhinol Laryngol* 1976;85:169–184.
16. Engstrom B, Hillerdal M, Laurell G, Bagger-Sjöback D. Selected pathological findings in the human cochlea. *Acta Otolaryngol (Stockh)* 1987;436:110–116.
17. Jennings CR, Jones NS. Presbycusis. *J Laryngol Otol* 2001; 115:171–178.
18. Gates GA, Mills JH. Presbycusis. *Lancet* 2005;366:1111–1120.
19. Nelson EG, Hinojosa R. Presbycusis: a human temporal bone study of individuals with flat audiometric patterns of hearing loss using a new method to quantify stria vascularis volume. *Laryngoscope* 2003;113:1672–1686.
20. Kusunoki T, Cureoglu S, Schachern PA, et al. Age-related histopathologic changes in the human cochlea: a temporal bone study. *Otolaryngol Head Neck Surg* 2004;131: 897–903.
21. Rüttiger L, Panford-Walsh R, Schimmang T, et al. BDNF mRNA expression and protein localization are changed in age related hearing loss. *Neurobiol Aging* 2006 March 29; Epub ahead of print.

ARTICLE

doi:10.1016/j.ymthe.2006.06.012

# Cell–Gene Delivery of Brain-Derived Neurotrophic Factor to the Mouse Inner Ear

Takayuki Okano, Takayuki Nakagawa,* Tomoko Kita, Tsuyoshi Endo, and Juichi Ito

*Department of Otolaryngology–Head and Neck Surgery, Graduate School of Medicine, Kyoto University, 606-8507 Kyoto, Japan*

**To whom correspondence and reprint requests should be addressed at the Department of Otolaryngology–Head and Neck Surgery, Graduate School of Medicine, Kyoto University, Kawaharacho 54, Shogoin, Sakyo-ku, 606-8507 Kyoto, Japan. Fax: +81 75 751 7225. E-mail: tnakagawa@ent.kuhp.kyoto-u.ac.jp.*

Available online 7 September 2006

**Sensorineural hearing loss is a common disability, but treatment options are currently limited to cochlear implants and hearing aids. Studies are therefore being conducted to provide alternative means of biological therapy, including gene therapy. Safe and effective methods of gene delivery to the cochlea need to be developed to facilitate the clinical application of these therapeutic treatments for hearing loss. In this study, we examined the potential of cell–gene therapy with nonviral vectors for delivery of therapeutic molecules into the cochlea. NIH3T3 cells were transfected with the brain-derived neurotrophic factor (*Bdnf*) gene using lipofection and then transplanted into the mouse inner ear. Immunohistochemistry and Western blotting demonstrated the survival of grafted cells in the cochlea for up to 4 weeks after transplantation. No significant hearing loss was induced by the transplantation procedure. A Bdnf-specific enzyme-linked immunosorbent assay revealed a significant increase in Bdnf production in the inner ear following transplantation of engineered cells. These findings indicate that cell–gene delivery with nonviral vectors may be applicable for the local, sustained delivery of therapeutic molecules into the cochlea.**

**Key Words: gene therapy, cell transplantation, hearing loss, cochlea, brain-derived neurotrophic factor, nonviral vector**

## INTRODUCTION

Sensorineural hearing loss (SNHL) is one of the most common disabilities in industrialized countries. Defects in the auditory hair cells, and in their associated spiral ganglion neurons (SGNs), can lead to hearing loss or deafness. Approximately 50% of SNHL cases have a genetic basis, a significant proportion of which is non-syndromic and usually inherited in an autosomal recessive manner [1]. In the past decade, many genetic mutations that cause deafness have been identified, which may contribute to the biological sources available for therapeutic approaches. Should the restoration of mutated genes in the cochlea by gene manipulation become a reality, gene therapy might be a promising method for treating SNHL of genetic origin.

Protecting auditory hair cells and SGNs from irreversible degeneration is a primary objective as inner ear cells have limited regeneration capacity. With the recent increase in understanding of the role of neurotrophic factors, including brain-derived neurotrophic factor (BDNF), on the maintenance of the mature peripheral auditory systems, there have been numerous attempts to define ways to reduce hair cell and SGN degeneration [2–6]. Since neurotrophins have a short serum half-life of just minutes or hours [7], their sustained local delivery is essential for cochlear protection. Previous studies have used viral vectors, particularly adenoviruses or adeno-associated viruses, to deliver neurotrophins to the cochleae [8–13]. However, despite their high transduction efficiency, high titer, and ease of production, viral vectors involve potential toxicity.

Gene therapy could enable the long-term delivery of several agents into the inner ear. Cell transplantation has been used as a means of delivering peptides or proteins into the central nervous system, demonstrating its use as a delivery vehicle for therapeutic molecules [14–16]. In addition, recent studies have demonstrated successful cell transplantation into the mouse cochlea [17,18]. Therefore, transplantation of cells that have been genetically manipulated *in vitro* using nonviral vectors potentially resolves the problem of viral vector toxicity in cochlear gene therapy.

In this study, we conducted an examination of the efficiency of cell–gene delivery into the cochlea for application of therapeutic molecules to the treatment of SNHL. We chose NIH3T3 cells as a delivery vehicle for the



1525-0016/$30.00

gene. NIH3T3 cells are a well-established fibroblast cell line, so that it is easy to optimize conditions for gene transfer and to select gene-expressing cells *in vitro*. In addition, fibroblasts are available from various human sources, which may be advantage for extending future clinical investigations. We transfected NIH3T3 cells with the *Bdnf* gene using lipofection. We then examined the potential for transplanting transfected NIH3T3 cells into the mouse inner ear.

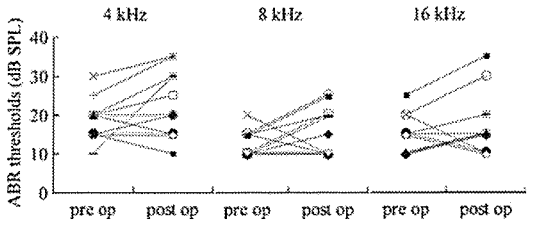


FIG. 1. ABR thresholds before and after cell transplantation. The left lane shows preoperative (pre op) ABR thresholds of each ear, and the right shows those recorded on day 28 after transplantation (post op) at 4, 8, and 16 kHz. The *x* axis shows ABR thresholds (dB SPL).

## Results and Discussion

### *Bdnf* Gene Transfer

To determine the efficacy of gene transfection using a nonviral vector, we performed reverse transcriptase-polymerase chain reaction (RT-PCR) analysis of Bdnf mRNA levels in transfected and nontransfected NIH3T3 cells (data not shown). NIH3T3 cells transfected with the mouse *Bdnf* gene (NIH3T3/BDNF) demonstrated Bdnf mRNA expression (86-bp fragment), which was absent from cells transfected with a vector carrying an antibiotic resistance gene (NIH3T3/control) and from nontransfected cells (NIH3T3/original). Amplification of gylceraldehyde-3-phosphate dehydrogenase (*Gapdh*), yielding a 171-bp amplicon, was used as an internal control. Negative control reactions that lacked reverse transcriptase failed to yield amplicons of either *Gapdh* or *Bdnf*.

We carried out an enzyme-linked immunosorbent assay (ELISA) for Bdnf protein to examine the efficacy of Bdnf protein expression and secretion *in vitro*. The mean Bdnf concentration in the culture medium of NIH3T3/BDNF cells, at 396.70 ± 32.66 pg/ml, was significantly higher than in the medium of either NIH3T3/control cells (24.96 ± 5.22 pg/ml) or NIH3T3/original cells (32.42 ± 7.09 pg/ml) ($P < 0.0001$). These findings demonstrate efficient, functional gene transfer into NIH3T3 cells *in vitro* by a liposome-mediated delivery method.

### Cell Transplantation into Mouse Cochleae

We transfected NIH3T3 cells with the mouse *Bdnf* gene tagged with a FLAG epitope (NIH3T3/FLAG) to enable transfected, transplanted cells to be readily distinguished from host inner ear cells. We injected suspensions of NIH3T3/FLAG and NIH3T3/control cells into the perilymphatic space of the posterior semicircular canal of C57BL/6 mice using a technique that we developed in previous studies [17,18]. Although delivery of cells into the mouse cochlea is difficult because of its small size, the well-defined genetics of a mouse model enable a variety of analyses of the inner ear to be performed.

We performed auditory brain stem response (ABR) recording to evaluate the effects of the transplantation procedure on hearing (Fig. 1). Alterations in ABR thresholds between pre- and postoperation were limited within 10 dB, although one animal exhibited a 20-dB elevation in ABR thresholds at 4 kHz. Preoperative ABR thresholds were 18.6 ± 1.7 (dB SPL) at 4 kHz, 12.7 ± 1.0 at 8 kHz, and 15.5 ± 1.4 at 16 kHz, and those on postoperative day 28 were 22.7 ± 2.6 at 4 kHz, 15.9 ± 1.9 at 8 kHz, and 17.3 ± 2.5 at 16 kHz. We identified no significant elevation of ABR thresholds on day 28 at frequencies of 4, 8, and 16 kHz. In addition, we observed no vestibular dysfunction in the behavior of the animals after the operation. These findings indicate the limited surgical invasiveness of our transplantation procedure, which is almost identical to previous observations [19,20].

Immunohistochemical analysis of FLAG expression demonstrated the settlement and survival of grafted NIH3T3/FLAG cells in both the cochlea and the vestibule (Figs. 2A, 2B, 2D, 2E). The engrafted cells were clearly distinct from the endogenous cells based on their expression of FLAG, while control specimens that were transplanted with NIH3T3/control cells exhibited no expression of FLAG (Figs. 2C and 2F). Grafted cells were localized in the perilymphatic space of cochleae or vestibules and did not establish in the endolymphatic space or within the inner ear tissues. These locations are identical to those of neural stem cell-derived cells transplanted into the mouse inner ear through the semicircular canal in our previous study [17]. On day 7, we found numerous grafted cells as cell aggregates in the vestibule. On day 28, we still observed grafted cells in both vestibules and cochleae, but did not see aggregation of grafted cells. Of grafted cells located in the perilymphatic space of cochleae, 91.2 ± 11.1% adhered to host cochlear tissues on day 7 and 92.3 ± 14.7% on day 28. The survival and settlement of grafted cells in the inner ear were also demonstrated by Western blotting for FLAG (Fig. 2G). We prepared protein lysates from the inner ear specimens obtained on day 28. The FLAG-tagged *Bdnf* transgene product (31 kDa) was detected in specimens transplanted with NIH3T3/FLAG cells, but not in those transplanted with NIH3T3/control cells. The β-actin internal control was detected in both specimens at equal density. These findings demonstrate that cells transplanted through the posterior semicircular canal survive and produce gene-encoded proteins in the perilymphatic space of cochleae and vestibules, indicating

doi:10.1016/j.ymthe.2006.06.012




**FIG. 2.** Localization of grafted NIH3T3/FLAG cells in the inner ear and infiltration of CD45-positive cells in cochleae. (A–F) Grafted cells are labeled with FLAG (green fluorescence), and cell nuclei are labeled with DAPI (blue fluorescence). A number of grafted cells are found both in the cochlea (A) and in the vestibule (D) at 1 week after transplantation. In the vestibule, numerous grafted cells form cell aggregates (D). Grafted cells are also identified in the cochlea (B) and vestibule (E) at 4 weeks after transplantation. No FLAG-positive cells were found in the control cochlea (C) or vestibule (F). Bars represent 200 μm and 20 μm in insets. (G) Western blot for FLAG expression in the inner ear at 4 weeks after cell transplantation. The FLAG-tagged Bdnf (31-kDa band) is detected in cochleae engrafted with NIH3T3/BDNF-FLAG cells (lane 1), but not in engrafted control cells (lane 2). β-Actin (42-kDa band), an internal control, is detected in both specimens at the same density. (H–J) Localization of CD45-positive cells in cochleae. In control cochleae, CD45-positive cells (red fluorescence) are found in the spiral ligament and spiral ganglion (arrows in H). CD45-positive cells were localized in the spiral ganglion, osseous spiral lamina, spiral ligament, and spiral limbus (arrows) at 1 (I) and 4 weeks (J) after engraftment of NIH3T3/BDNF-FLAG cells. Blue fluorescence shows DAPI. Bars represent 200 μm.

sustained delivery of Bdnf from transplanted cells to the perilymphatic space of the inner ears. Previous investigations have demonstrated that application of neurotrophins, including Bdnf, into the perilymph efficiently protects hair cells or spiral ganglion neurons from various ototoxic insults [2–6,10,11], indicating that neurotrophins delivered in the perilymph act on hair cells and spiral ganglion neurons. We therefore consider that Bdnf secreted from transplanted cells may be accessible to hair cells and spiral ganglion neurons.

The numbers of FLAG-positive cells in the cochlea decreased from the time point of day 7 to that of day 28. On day 7 after transplantation, we observed $26.7 \pm 3.3$ grafted cells in one midmodiolus section of cochleae, while we found $14.4 \pm 2.3$ cells on day 28. We then analyzed infiltration of inflammatory cells into cochlear tissues to investigate immune-mediated clearance of grafted cells. We employed immunohistochemistry for CD45, a leukocyte common antigen, to determine the distribution of inflammatory cells in the cochlea. In control cochleae, we found CD45-positive cells in the spiral ganglion, spiral limbus, and spiral ligament (Fig. 2H). Cochleae that received transplantation of NIH3T3/FLAG cells exhibited a similar distribution of CD45-positive cells compared to that of control cochleae (Figs. 2I and 2J). We observed no obvious infiltration of CD45-positive cells into the perilymphatic space of cochleae. These findings demonstrate that infiltration of inflammatory cells is not induced by transplantation of NIH3T3/FLAG cells into the inner ears. Even after xenografts into the cochlear fluid space without use of immune suppressants, cell infiltration into the cochlear fluid space has not been observed [21]. We therefore consider that immune-mediated clearance may not play a central role in elimination of transplanted cells from the inner ear. However, further studies are required to determine actual roles of the immune system in the decrease in transplanted cells in the inner ears.

### Efficiency of Gene Delivery

We performed an ELISA of Bdnf proteins extracted from the inner ear to examine the efficiency of cell–gene delivery. We collected the inner ear specimens on day 7 after transplantation and calculated the ratio of Bdnf concentration to total protein in the sample solutions. NIH3T3/BDNF cell-transplanted specimens showed a significantly higher ratio ($93.40 \pm 10.69$ pg/mg total protein) compared with NIH3T3/control cell-transplanted samples ($46.68 \pm 4.41$ pg/mg) ($P = 0.01$). There was no significant difference between the levels of total protein extracted from the two samples (NIH3T3/BDNF, $2.65 \pm 0.21$ mg/ml; NIH3T3/control, $2.77 \pm 0.12$ mg/ml). These findings demonstrate that Bdnf synthesis by engrafted NIH3T3/BDNF cells contributes to a significant increase in Bdnf protein levels of the inner ear specimens, suggesting that cell–gene therapy may be applicable for local, sustained delivery of therapeutic molecules into the inner ear.

This is the first report that demonstrates the successful cell–gene delivery of therapeutic molecules to the cochlea without the use of viral vectors, an encouraging result for the extension of research into gene therapy for the inner ear. Currently, several experiments utilize human fibroblasts as a delivery vehicle [22,23]. The use of autologous bone marrow-derived stromal cells for transplants into the inner ear has been reported [24]. Such cells eliminate the risk of immunoresponses, and their ability to migrate into the cochlear lateral wall and modiolus is likely to enhance the potential for delivery of genes into these areas of the cochlea. Future studies should be performed to evaluate the potential of these alternative transplant media as a vehicle for gene delivery.

In summary, we transplanted NIH3T3 cells that had been genetically engineered to express Bdnf into the mouse inner ear and evaluated the efficiency of transplantation for local delivery of gene products. The results demonstrated a significant increase in Bdnf protein in the inner ear following transplantation of engineered cells. These findings indicate that gene therapy may be a feasible treatment option for inner ear diseases such as SNHL. Cell–gene delivery of therapeutic molecules into the inner ear is suitable for protection of inner ear cells against gradually progressive degeneration. Presbycusis, age-related hearing loss, may be included in targets for cell–gene therapy. BDNF application via cell–gene delivery could be an efficient strategy for promotion of survival of SGNs in cases of cochlear implants (CIs), which are small devices that are surgically implanted in the cochlea to stimulate SGNs. BDNF transgene produced by gene-engineered cells will support the survival of SGNs after CI surgery, which can contribute to the maintenance of hearing benefits provided by CIs.

## Materials and Methods

***Animals.*** Forty-three 10-week-old male C57BL/6 mice (SLC Japan, Hamamatsu, Japan) with normal hearing were used in the study. All mice were maintained in the Institute of Laboratory Animals, Kyoto University Graduate School of Medicine. All experimental protocols were approved by the Animal Research Committee, Kyoto University Graduate School of Medicine, and conducted in accordance with NIH guidelines for the care and use of laboratory animals.

***Vector construction.*** The *Mus musculus* (house mouse) brain-derived neurotrophic factor cDNA clone (GenBank Accession No. BC034862) was obtained from Invitrogen (Carlsbad, CA, USA). PCR amplification of the cDNA using Pyrobest DNA polymerase (TaKaRa-Bio, Kyoto, Japan) was performed with the following primer pairs: 5′ primer, 5′-GGAATTCGCCACCATGACCATCCTTTTCCTTACTATGG-3′; 3′ primer 1, 5′-ATAAGAATAAGCGGCCGCTCATCTTCCCCTTTTAATGGTCAGTG-3′; and 3′ primer 2, incorporating two pairs of FLAG epitope, 5′-ATAAGAATAAGCGGCCGCTCACTTGTCATCGTCGTCCTTGTAGTCCTTGTCATCGTCGTCCTTGTAGTCCTTGTCATCGTCGTCCTTGTAGTCTCTTCCCCTTTTAATGGTCAGTG-3′. PCR products were digested with *Eco*RI and *Not*I, and a 0.77-kb

doi:10.1016/j.ymthe.2006.06.012

*Eco*RI–*Not*I fragment containing mouse *Bdnf* or mouse *Bdnf* with FLAG epitope was cloned into the *Eco*RI–*Not*I site of the pIRESneo3 vector (BD Biosciences, Palo Alto, CA, USA) using Ligation Solution (TaKaRa-Bio) to generate plasmid pIRESneo3-bdnf (supplementary information) or pIRESneo3-bdnfflag. For subsequent experiments, plasmid pIRESneo3 containing the neomycin-resistant gene only (pIRESneo3-control) was also amplified. Restriction analysis and DNA sequencing were used to confirm the integrity of all constructs.

***Cell lines and gene transfer.*** NIH3T3 cells were obtained from Riken Cell Bank (RCB 0150; Tsukuba, Japan) and cultured in Dulbecco's modified Eagle's medium (DMEM; GIBCO BRL, Grand Island, NY, USA) containing 10% newborn calf serum (GIBCO), penicillin (100 U/ml), streptomycin (100 μg/ml), and amphotericin B (0.25 μg/ml) in a humidified atmosphere of 5% $CO_2$ at 37°C. NIH3T3 cells were plated at a density of $1 \times 10^5$ cells per 100-mm plastic dish and incubated for 48 h. Transfection was performed with 18 μl of FuGENE6 Transfection Reagent (Roche, Indianapolis, IN, USA) complexed with 9 μg pIRESneo3-bdnf, pIRESneo3-bdnfflag, or pIRESneo3-control plasmid in DMEM per 100-mm plastic dish at 37°C for 6 h. The medium was then replaced with conditioned medium containing Geneticin sulfate (G418; Sigma, St. Louis, MO, USA) for the selection of stably transfected cell clones.

***Bdnf mRNA expression in cell lines.*** The expression of Bdnf mRNA in the cell lines was analyzed with RT-PCR. Total RNA was extracted from the cultured cell lines using the RNeasy Kit (Qiagen GmbH, Germany) and then treated with DNase I (Ambion, Austin, TX, USA). Four sets of total RNA for each cell line were prepared. PCRs were performed using TaqMan Gold PCR Master Mix (Applied Biosystems, Foster City, CA, USA) and Bdnf-specific primers. Gapdh mRNA was used as the invariant control. All reactions were performed in triplicate.

***Bdnf secretion from cell lines.*** Bdnf protein levels in culture medium were measured by ELISA to examine Bdnf secretion by transfected cells. NIH3T3/BDNF, NIH3T3/control, and NIH3T3/original cells ($1 \times 10^5$) were inoculated in 60-mm plastic dishes with 3 ml conditioned medium. The supernatants of the conditioned media were harvested approximately 24 h after inoculation. ELISA was performed using the BDNF Emax Immunoassay System (Promega, Madison, WI, USA) according to the manufacturer's instructions. Four sets of samples were prepared from each cell line, and all reactions were performed in triplicate.

***Cell transplantation.*** On the day of transplantation, cultured cells were suspended at $3 \times 10^4$ cells/μl DMEM/F12 (GIBCO). NIH3T3/BDNF cells were transplanted into 10 animals, NIH3T3/FLAG cells into 24 animals, and NIH3T3/control cells into 9 animals. Cell transplantation was performed under general anesthesia with 75 mg/kg ketamine and 9 mg/kg xylazine. A retroauricular incision was made in the left ear, and the posterior semicircular canal (PSCC) was exposed. A small hole was made in the bony wall of the PSCC. A fused silica glass needle (EiCOM, Kyoto, Japan) was then inserted into the perilymphatic space of the PSCC, and the cell suspension was injected at the rate of 1 μl/min for 3 min using a Micro Syringe Pump (EiCOM).

***Measurement of auditory function.*** The auditory function of experimental animals was monitored by ABR recording. ABR measurements were performed as previously described [25]. ABRs were recorded before cell transplantation and on day 28 in the 11 animals that received an engraftment of NIH3T3/FLAG cells. Thresholds were determined for frequencies of 4, 8, and 16 kHz.

***Immunohistochemistry.*** Under general anesthesia, the animals that had been engrafted with NIH3T3/BDNF-FLAG cells were transcardially perfused with phosphate-buffered saline, pH 7.4, followed by 4% paraformaldehyde in phosphate buffer at pH 7.4 on day 7 ($n=10$) or 28 ($n=10$). Immediately, the temporal bones were dissected out and immersed in the same fixative for 4 h at 4°C. Specimens were prepared as cryostat sections. Two midmodiolus sections were chosen from each specimen and stained by immunohistochemistry for FLAG to distinguish transplanted cells from host specimens. Two cochleae on day 7 after transplantation of NIH3T3/control cells were used as controls for immunostaining for FLAG. We counted the numbers of FLAG-positive cells and those of FLAG-positive cells that adhered to cochlear tissues. The ratios of grafted cell that adhered to cochlear tissues were then calculated. The emergence of CD45-positive cells was also examined to evaluate inflammatory response following cell transplantation. Untreated cochlear specimens were served as controls for immunostaining for CD45. Anti-FLAG M2 mouse monoclonal antibody (1:230; Sigma) or anti-mouse CD45 rat monoclonal antibody (a leukocyte common antigen, Ly-5, 1:20; BD PharMingen, San Diego, CA, USA) was used as the primary antibody, and FITC-conjugated goat anti-mouse antibody (1:500; Santa Cruz Biotechnology, Santa Cruz, CA, USA) or Alexa-Fluor 546-conjugated anti-rat antibody (1:500; Molecular Probes, Eugene, OR, USA) was used as the secondary antibody. Counterstaining by 4′,6-diamidino 2-phenylindole dihydrochloride (DAPI; 1 μg/ml; Molecular Probes) was performed to demonstrate nuclear locations.

***FLAG Western blotting.*** The expression of FLAG-tagged Bdnf fusion protein in the inner ear engrafted with NIH3T3/FLAG cells ($n=4$) or NIH3T3/control cells ($n=4$) was determined by Western blotting 28 days after transplantation. The temporal bones were homogenized in ice-cold lysis buffer. After centrifugation of the homogenized solution, the supernatants were assayed for proteins. The sample solutions were electroblotted onto a polyvinyldifluoride membrane. The primary antibody was a mouse monoclonal anti-FLAG antibody (1:500; Sigma) or rabbit polyclonal anti-β-actin antibody (1:200; Sigma), and the secondary antibody was HRP-conjugated anti-mouse IgG (1:50,000; Amersham Biopharmacia Biotech, Buckinghamshire, UK) or anti-rabbit IgG (1:25,000; Amersham Biopharmacia Biotech). Reactions were visualized by chemiluminescence using an ECL Plus Western blotting reagent pack (Amersham Biopharmacia Biotech).

***Measurement of Bdnf levels in the inner ear.*** To assess the *in vivo* production of Bdnf protein by grafted cells, the inner ears engrafted with NIH3T3/BDNF cells ($n=10$) or NIH3T3/control cells ($n=5$) were removed on day 7 after transplantation. A Bdnf ELISA was performed using the BDNF Emax Immunoassay System (Promega) according to the manufacturer's protocol. All reactions were performed in triplicate. Total protein concentration was measured with the Lowry assay using the Bio-Rad DC Protein Assay (Bio-Rad, Hercules, CA, USA).

***Statistical analysis.*** Results were expressed as means ± standard error. Statistical analyses for Bdnf levels in the cultured medium and ABR threshold shifts were performed using one-way ANOVA followed by Sheffe's multiple-comparison tests. A Mann–Whitney *U* test was used to compare cochlear Bdnf levels. Probability (*P*) values less than 5% were considered significant.

## ACKNOWLEDGMENTS

*The authors thank Daisuke Yabe and Norio Yamamoto (Department of Medical Chemistry and Molecular Biology, Kyoto University Graduate School of Medicine, Japan) for help and instruction with molecular biology, Junko Okano (Department of Anatomy and Developmental Biology, Kyoto University Graduate School of Medicine) for critical discussion, and Yoko Nishiyama and Rika Sadato for their technical assistance. This study was supported by a Grant-in-Aid for Scientific Research (B2, 16390488, 2004–2006, T.N.) from the Ministry of Education, Culture, Sports, Science, and Technology of Japan and in part by a grant (2005–2006, T.N.) from the Takeda Science Foundation and a grant (2005, T.O.) from the 21st Century COE Program of the Ministry of Education, Culture, Sports, Science, and Technology of Japan.*

RECEIVED FOR PUBLICATION MARCH 7, 2006; REVISED JUNE 8, 2006; ACCEPTED JUNE 21, 2006.

## APPENDIX A. SUPPLEMENTARY DATA

Supplementary data associated with this article can be found, in the online version, at doi:10.1016/j.ymthe.2006.06.012.

## REFERENCES


1. Nance, W. E. (2003). The genetics of deafness. *Ment. Retard. Dev. Disabil. Res. Rev.* **9:** 109–119.
2. Altschuler, R. A., Cho, Y., Ylikoski, J., Pirvola, U., Magal, E., and Miller, J. M. (1999). Rescue and regrowth of sensory nerves following deafferentation by neurotrophic factors. *Ann. N.Y. Acad. Sci.* **884:** 305–311.
3. Gillespie, L. N., Clark, G. M., Bartlett, P. F., and Marzella, P. L. (2003). BDNF-induced survival of auditory neurons in vivo: cessation of treatment leads to accelerated loss of survival effects. *J. Neurosci. Res.* **71:** 785–790.
4. Endo, T., *et al.* (2005). Novel strategy for treatment of inner ears using a biodegradable gel. *Laryngoscope* **115:** 2016–2020.
5. Noushi, F., Richardson, R. T., Hardman, J., Clark, G., and O'Leary, S. (2005). Delivery of neurotrophin-3 to the cochlea using alginate beads. *Otol. Neurotol.* **26:** 528–533.
6. Shinohara, T., *et al.* (2002). Neurotrophic factor intervention restores auditory function in deafened animals. *Proc. Natl. Acad. Sci. USA* **99:** 1657–1660.
7. Kishino, A., *et al.* (2001). Analysis of effects and pharmacokinetics of subcutaneously administered BDNF. *Neuroreport* **12:** 1067–1072.
8. Staecker, H., Gabaizadeh, R., Federoff, H., and Van De Water, T. R. (1998). Brain-derived neurotrophic factor gene therapy prevents spiral ganglion degeneration after hair cell loss. *Otolaryngol. Head Neck Surg.* **119:** 7–13.
9. Chen, X., Frisina, R. D., Bowers, W. J., Frisina, D. R., and Federoff, H. J. (2001). HSV amplicon-mediated neurotrophin-3 expression protects murine spiral ganglion neurons from cisplatin-induced damage. *Mol. Ther.* **3:** 958–963.
10. Yagi, M., Magal, E., Sheng, Z., Ang, K. A., and Raphael, Y. (1999). Hair cell protection from aminoglycoside ototoxicity by adenovirus-mediated overexpression of glial cell line-derived neurotrophic factor. *Hum. Gene Ther.* **10:** 813–823.
11. Hakuba, N., *et al.* (2003). Adenovirus-mediated overexpression of a gene prevents hearing loss and progressive inner hair cell loss after transient cochlear ischemia in gerbils. *Gene Ther.* **10:** 426–433.
12. Nakaizumi, T., Kawamoto, K., Minoda, R., and Raphael, Y. (2004). Adenovirus-mediated expression of brain-derived neurotrophic factor protects spiral ganglion neurons from ototoxic damage. *Audiol. Neurootol.* **9:** 135–143.
13. Stone, I. M., Lurie, D. I., Kelley, M. W., and Poulsen, D. J. (2005). Adeno-associated virus-mediated gene transfer to hair cells and support cells of the murine cochlea. *Mol. Ther.* **11:** 843–848.
14. Cejas, P. J., *et al.* (2000). Lumbar transplant of neurons genetically modified to secrete brain-derived neurotrophic factor attenuates allodynia and hyperalgesia after sciatic nerve constriction. *Pain* **86:** 195–210.
15. Cao, L., *et al.* (2004). Olfactory ensheathing cells genetically modified to secrete GDNF to promote spinal cord repair. *Brain* **127:** 535–549.
16. Girard, C., *et al.* (2005). Grafts of brain-derived neurotrophic factor and neurotrophin 3-transduced primate Schwann cells lead to functional recovery of the demyelinated mouse spinal cord. *J. Neurosci.* **25:** 7924–7933.
17. Iguchi, F., *et al.* (2003). Trophic support of mouse inner ear by neural stem cell transplantation. *Neuroreport* **14:** 77–80.
18. Tateya, I., *et al.* (2003). Fate of neural stem cells grafted into injured inner ears of mice. *Neuroreport* **14:** 1677–1681.
19. Iguchi, F., *et al.* (2004). Surgical techniques for cell transplantation into the mouse cochlea. *Acta Otolaryngol. Suppl.* **551:** 43–47.
20. Kawamoto, K., Oh, S. H., Kanzaki, S., Brown, N., and Raphael, Y. (2001). The functional and structural outcome of inner ear gene transfer via the vestibular and cochlear fluids in mice. *Mol. Ther.* **4:** 575–585.
21. Hildebrand, M. S., *et al.* (2005). Survival of partially differentiated mouse embryonic stem cells in the scala media of the guinea pig cochlea. *J. Assoc. Res. Otolaryngol.* **6:** 341–354.
22. Evans, C. H., *et al.* (2005). Gene transfer to human joints: progress toward a gene therapy of arthritis. *Proc. Natl. Acad. Sci. USA* **102:** 8698–8703.
23. Kakeda, M., *et al.* (2005). Human artificial chromosome (HAC) vector provides long-term therapeutic transgene expression in normal human primary fibroblasts. *Gene Ther.* **12:** 852–856.
24. Naito, Y., *et al.* (2004). Transplantation of bone marrow stromal cells into the cochlea of chinchillas. *Neuroreport* **15:** 1–4.
25. Shiga, A., *et al.* (2005). Aging effects on vestibulo-ocular responses in C57B/6 mice: comparison with alteration in auditory function. *Audiol. Neurootol.* **10:** 97–104.

*Otology & Neurotology*
27:592–595 © 2006, Otology & Neurotology, Inc.

# A New Tool for Testing Ossicular Mobility During Middle Ear Surgery: Preliminary Report of Four Cases

*Naohito Hato, *Hisashi Kohno, *Masahiro Okada, *Nobuhiro Hakuba, *Kiyofumi Gyo, †Takashi Iwakura, and †Makoto Tateno

**Department of Otolaryngology, Ehime University School of Medicine, Ehime; and †Rion Co., Ltd., Tokyo, Japan*

**Objective:** We developed an ossicular vibration tester for the objective and quantitative assessment of ossicular mobility, which is one of the most critical factors affecting postoperative hearing after tympanoplasty.

**Methods:** Our device consists of three components: a probe shaft with a curved tip to be attached to the target ossicle, a vibration exciter to activate the probe, and a piezoelectric sensor to detect vibrations of the probe. These components are encased in a stainless steel holder, allowing easy hand manipulation during ear surgery. The probe is activated with an electric signal at around 1,600 Hz. The system is controlled with a laptop computer, and the results are presented as the ratio of the ossicular resistance (ROR) to a reference value as a percentage. One measurement takes 10 ms. The device was applied in four selected patients during ear surgery.

**Results:** Several measurements in two of the cochlear implantees showed a greater difference in the RORs of the stapes (15–20% in Case 1 and 35–45% in Case 2), whereas the RORs of the malleus and incus were within the same range. This was thought to correspond to the partial cochlear calcification noted in Case 2. In Case 3, who underwent surgery because of otosclerosis, the ROR of the stapes was high, ranging from 70 to 80%. When measured for the malleus-incus fixation anomaly (Case 4), the ROR of the malleus and incus was in the range of 60 to 70%. Owing to the limited surgical view, the ROR of the stapes could not be measured. No problems related to the measurements with this device were noted.

**Conclusion:** The design, principles, measuring procedures, and preliminary results of our new tool for testing ossicular mobility are reported. Measuring the ossicular mobility during surgery may provide important information for deciding the surgical procedures. **Key Words:** Ossicular mobility—Otosclerosis—Postoperative hearing—Tympanoplasty—Vibration tester.

*Otol Neurotol* **27**:592–595, 2006.

Hearing does not always improve satisfactorily after tympanoplasty. The outcome depends on a variety of factors such as middle ear disease, tubal function, the surgeon's skill, and the type of ossicular reconstruction. The mobility of the ossicles, especially of the stapes, is thought to be one of the most critical factors affecting postoperative hearing (1). When stapes fixation is observed in surgery for chronic otitis media, conventional tympanoplasty is usually insufficient to restore hearing, even when the inflammatory disease is eradicated. Good hearing is expected only when the mobility of the stapes remains intact or is improved by the surgical procedure. Most otologic surgeons assess the ossicular mobility by placing an ear pick on the ossicle and activating it manually. This maneuver provides only a rough estimate, and the results are subjective.

In 1963, Lau et al. (1) reported an ossicular mobility checker called Schallsonde, but the device did not become popular because its clinical significance was not fully recognized at the time. In 1997, we developed an ossicular vibration tester using a pair of ceramic elements (2,3). Although it provided important information on ossicular mobility, clinical assessment of the device revealed the following intrinsic drawbacks:

1. the ceramic tip was so fragile that it could not tolerate hard use during surgery;
2. the device had to be held stable with its tip in contact with the ossicle for 8 s;
3. measurements were often influenced by electric noise in the operating room; and
4. many additional instruments were required, such as an electric stimulator, amplifier, and spectrum analyzer.

Address correspondence and reprint requests to Naohito Hato, M.D., Department of Otolaryngology, Ehime University School of Medicine, Shitsukawa To-on City, Ehime 791-0295, Japan; E-mail: nhato@m.ehime-u.ac.jp

In 2001, Wada et al. (4) introduced a new measuring system using a single ceramic element and a micropressure sensor to evaluate stapes mobility. Although the system seemed promising, they had applied it only in guinea pigs and rabbits, suggesting that a clinical trial of their system seemed premature.

Recently, we developed a new ossicular mobility tester using an electromagnetic driver and a piezoelectric sensor. The probe is small enough to be manipulated easily during ear surgery, taking advantage of its handheld design (Fig. 1). The handpiece is reusable after ethylene oxide gas sterilization. The device is a computer-controlled system, and it overcomes most of the drawbacks of our previous system. This article reports the structure, principles, and measuring procedures for our new tool and shows preliminary results in four patients.

## PRINCIPLES OF THE MEASURING DEVICE

The ossicular vibration tester consists of three components, as shown in Figure 2: a pair of probe shafts with one end designed to be attached to a target ossicle, a piezoelectric force sensor incorporated between the probe shafts, and a vibration exciter for activating the probe shafts. The probe shaft is composed of stainless steel, with a diameter of 3.0 mm and bends at a 20-degree angle 20 mm from the tip. It tapers toward the tip, where it is shaped like a ball with a diameter of 0.5 mm. Except for the probe shaft, all of these components are encased in a handheld stainless steel holder. The moving parts, including the probe shaft, tip, and sensor, are suspended with springs. An exciter consisting of a moving-coil–type electromagnetic transducer makes the probe shaft vibrate along its long axis. Under the control of a laptop computer, the vibration exciter makes the probe shaft vibrate at the resonance frequency, which is around 1,600 Hz. When the vibration exciter is activated, a force sensor picks up the vibration of the shaft tip and transforms it into an electric signal. On activating the exciter with the shaft tip attached to a target ossicle, the output voltage

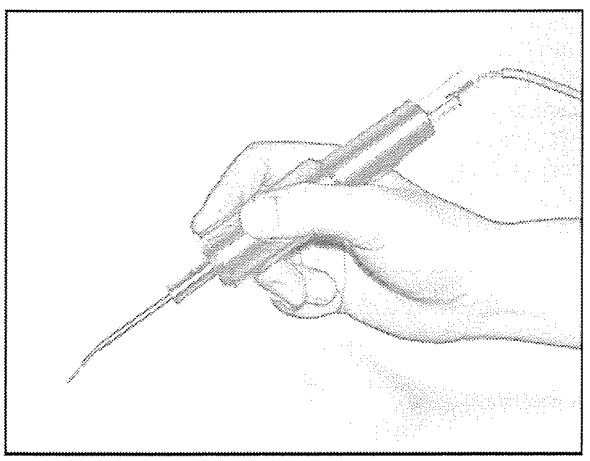

**FIG. 1.** The handheld ossicular mobility tester.

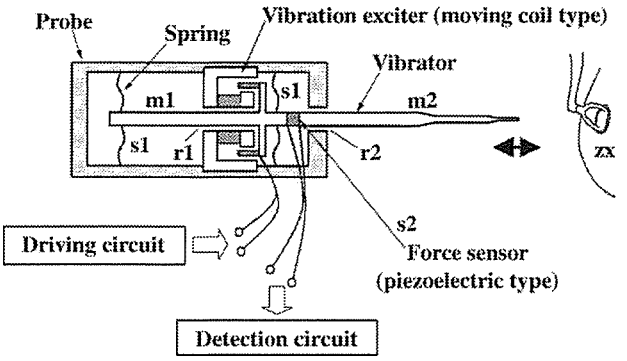


**FIG. 2.** Schema of the measuring system.

from the sensor changes in relation to the magnitude of the ossicular resistance. Therefore, by measuring both with the tip free of load and with it attached to an ossicle, we can calculate the mechanical impedance of the ossicle, which is thought to correspond to the inverse of the ossicular mobility. The details of the principle of this measuring device were reported in association with our previous article (5).

## MEASUREMENTS

All the measuring procedures were performed under an operating microscope to avoid damaging the inner ear. After exposure of the auditory ossicles, the tester was handheld at an appropriate angle, and baseline data were obtained via activating the probe without touching the tip to the ossicle. This procedure is important for tuning the vibration mode of the exciter, which varies with the angle of the handpiece to the target. The tip of the shaft was carefully placed on the ossicle, and the probe was activated with an electric signal (Fig. 3). One measurement took only 10 ms. The data were analyzed by sampling 512 points, and the dispersion of the data was calculated. When the dispersion exceeded 10%, the data were rejected automatically. Afterward, consecutive steady-wave responses were used to assess ossicular mobility. The loading electric current to the probe was set to 0.15 mA, which caused reciprocal vibration of the shaft around 50 nm. The amplitude corresponded to the vibration of the stapes at 100 dB SPL at 1,600 Hz (6). The computer calculated the ratio of ossicular resistance (ROR) as a percentage of a reference value. A low percentage indicates a low resistance of the ossicle and good ossicular mobility, and a high percentage indicates the opposite.

## PATIENTS AND RESULTS

As a preliminary experiment, ossicular mobility was evaluated in four patients who agreed to undergo clinical testing during surgery. The institutional review board of Ehime University School of Medicine approved the

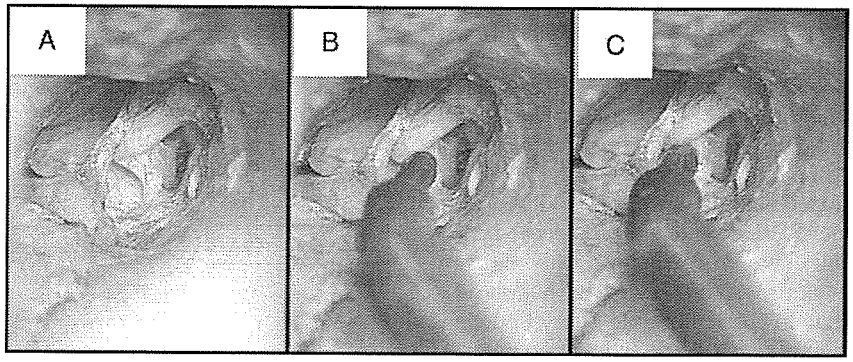


**FIG. 3.** Measuring procedure. Exposing the ossicles (*A*). Baseline measurement (*B*). Touching the probe tip to the side of the stapes head (*C*).

study design. Table 1 summarizes the patients' profiles, surgical procedures, and results of the measurements. Surgery and measurements were performed under general anesthesia in Patients 1 and 2 and under local anesthesia in Patients 3 and 4.

Patient 1 was a 45-year-old woman who had developed bilateral idiopathic sudden deafness 7 years earlier. At the time of cochlear implant surgery, the auditory ossicles seemed to move normally on manual manipulation. Ten measurements of each ossicle using the device gave RORs of 8 to 10%, 20 to 25%, and 15 to 20% for the malleus, incus, and stapes, respectively. All the active electrodes of the Nucleus 24 implant system (Cochlear Ltd., Lane Cove, Australia) were inserted.

Patient 2 was a 68-year-old man who underwent a cochlear implant for bilateral postmeningitic deafness that developed at age 10 years. His cochlea was partly ossified, and the ossicular mobility was somewhat reduced on manual manipulation using an ear pick. The RORs ranged between 25 and 35%, between 20 and 30%, and between 35 and 45% for the malleus, incus, and stapes, respectively. In this case, 12 of the 22 electrode arrays of the Nucleus 24 implant system could be inserted into the scala tympani.

Patient 3 was a 67-year-old woman with otosclerosis. The stapes was exposed via a transcanal approach, and the probe was carefully attached to the posterior side of the stapes head before disrupting the incudostapedial joint (Fig. 3). Manual manipulation of the ossicles revealed that the stapes was fixed. As expected, the ROR ranged from 70 to 80% on 10 successive measurements. After stapedotomy, the ossicle was reconstructed with a Teflon-piston wire, and the hearing result was excellent.

Patient 4 was an 18-year-old man. The malleus and incus were congenitally fixed to the surrounding bone, whereas the stapes moved normally. After exposure of the ossicles via the ear canal, the probe was applied to the malleus. In this case, the ROR ranged from 60 to 70%. Testing the mobility of the stapes was not feasible owing to the limited surgical field. No complications related to the measurements with this device were noted.

## DISCUSSION

The mobility of the auditory ossicle can be analyzed using a variety of equipment such as laser Doppler vibrometers (6,7), capacitive probes (8), and γ-ray counters (9,10). Most of these measuring systems can be applied only in the laboratory because of their size and the safety issues involved. Recently, laser Doppler vibrometer has been introduced in some otologic clinics as a tool for measuring ossicular mobility (11–13); however, it is still unpopular, mainly because of its high cost. Furthermore, it requires sound delivery equipment to activate the tympanic membrane, which often annoys the surgeon. Our device has several advantages over these devices: 1) it has a simple design and is handy and durable; 2) it is applicable even when the tympanic membrane has a perforation; 3) it does not need a sound delivery system; 4) ossicular mobility can be assessed in total or in part without disrupting the ossicular chain.

In this study, we measured the ROR as an indicator of ossicular mobility. According to Iwakura et al. (5), the ROR is correlated with the mechanical impedance of the target on a logarithmic scale; ROR values of 15, 45, and

**TABLE 1.** *Results of ossicular mobility in four patients*

| | Case 1 | Case 2 | Case 3 | Case 4 |
|---|---|---|---|---|
| Age (yr) sex | 45/female | 68/male | 67/female | 18/male |
| Diagnosis | Idiopathic deafness | Postmeningitis deafness | Otosclerosis | Congenital ossicular fixation |
| Surgery | Cochlear implant | Cochlear implant | Stapedotomy | Ossiculoplasty |
| Malleus (%) | 8–10 | 25–35 | NA | 60–70 |
| Incus (%) | 20–25 | 20–30 | NA | NA |
| Stapes (%) | 15–20 | 35–45 | 70–80 | NA |

NA, not applicable.